International Journal of Engineering &Technology, 7 (4) (2018) 6095-6104

International Journal of Engineering & Technology

Website: www.sciencepubco.com/index.php/IJET
doi: 10.14419/ijet.v7i4.23127
Research paper

Wavelet based Solar Cell Multilevel Diode Clamped Inverter in Induction Motor Computer Control

Mshari Aead AskerAlshammery [1] *, Wesam Ibrahim Hajim [2], Essa I Essa [3]

[1] Computer Department,Tikrit University,Iraq
[2] Department of Geology/Science Collge /Tikrit University
[3] College of Computer Science & IT/Kirkuk University/Iraq
**Corresponding author E-mail: dr.mshary.alshmmry@tu.edu.iq*

Abstract

The computer control is an essential stage of the any system verification. Wavelet as advanced signal processing technique due to its high performance and future extraction is used with implementation of incremental conductance maximum power point tracking (MPPT) technique. The MPPT is aimed to maximize the energy of photovoltaic (PV) energy conversion systems for induction motor (IM) operation. making them one of the cleanest power-generating technologies available. While they're operating, PV systems produce no air pollution, hazardous waste, or noise, and they require no transportable fuels. The fact that in the design phase of the photovoltaic systems which will feed electrical machines that the current drawn by any electrical machines at the start up is higher than the nominal operating current should be taken into account. Two wavelet techniques are used along with vector control to optimize the MPPT process performance, the first wavelet is Haar wavelet and the wavelet error obtained is acceptable but with new adaptive wavelet, optimal performance specification is obtained. The space vector pulse width modulation (SVPWM) based vector control is used to formulate excellent pulses of three level diode clamped inverter. In PV System, new set up is designed for the gate drive with F28335 DSP as computer control of the of the proposed algorithm. In this paper, the operating behaviors of 370W IM through a boost converter connected to PV system is equipped with integral controller for the duty cycle correction. Both the Computer simulation and experiment output results shows the effectiveness of the proposed algorithm of MPPT, SVPWM, wavelet and vector control with zero error and smooth operation for the IM current, speed and the DC voltage which ensure the effectiveness of the both boost converter and MPPT algorithm.

Keywords: *Solar Cell; Wavelet; Boost Converter; Maximum Power Point Tracking; Diode Clamped Inverter; Vector Control; IM.*

1. Introduction

The term computer control used in the industry when the computer is a part of the complete system. It doesn't mean the computer is working on but it may be mean a processor or microchip. The advance communication techniques as one of the signal processing topics plays an import role in the induction motors driven by photovoltaic cells (PV).Recently, PV array have obtained a great interest in many fields of industry due to energy recession. One of the most important objectives is to get maximum power point tracking (MPPT) for PV cells in any complete control system due its low efficiency [1].The wavelet is a new technique of signal processing used in various aspects to deal with signals in both time and frequency domains for feature extraction, increase the reliability, support MPPT and hence the efficiency of solar PV cells control system. Mathematically, It at various frequencies to group data and analysis capabilities with resolution study and subsequently matched components [2]. The MPPT can be used to reduced hardware setup. The junction conductance and the instantaneous conductance is used to realize the MPPT [3]. Advanced artificial neural network, fuzzy logic and bio techniques have been used to track the global MPPT during partial shading (PS) situations [4]. PV control system is illustrated in [5].A PV with low-cost pumping control system based on 3-φ induction motor (IM) is introduced in [6].Sliding mode(SM) power control based variable speed wind(VSW) energy conversion systems to maximize the power, reduce nonlinearities and external disturbances[7]. In any PV system, multiple peaks can be shown in the characteristic of power–voltage (P–V) [8]. Normally, the conventional MPPT that try to optimize results falls into local minimum. And need an improvement algorithms to overcome this situation [9]. The wavelet analysis as one of the advance signal processing techniques, the feature extraction with vector control IM drives is used efficiency of power generation control system. The Indirect Rotor-Field Oriented Control (IRFOC) techniques is used to control the single phase IM and centrifugal pump combination. The MPPT adjust pump operation to track the desired water flow and pressure conditions [10].

In the HV,HP energy control, multilevel inverter used frequently and the power semiconductor devices is most fragile in these industrial applications[11].The semiconductor junction temperature with the implementation in several emerging applications are presented in [12].

The digital signal processor (DSP) is presented widely to control the operation of IPMSM and any motor drive with or without PV control system [13].The ambient temperature and the insolation properties have to vary from the nominal operating point to reach the MPP of the PV array, hence both the PV array and the IM in the optimal response [14].

The main contribution of this paper are: using advance space vector pulse width modulation (SVPWM) communication technique to drive diode clamped multi-level inverter with vector control based wavelet technique as new signal processing feature extraction, build new adaptive wavelet group to obtain zero error for the

Copyright © 2018 Mshari Aead AskerAlshammery et al. This is an open access article distributed under the Creative Commons Attribution License, which permits unrestricted use, distribution, and reproduction in any medium, provided the original work is properly cited.

vector control IM drive and MPPT implementation with booster converter to stabilize the DC voltage of 370 W IM. The selection of the best solution is then found via DSPF28335 closed loop control system with minimum switching devices for IM gate drive.

The structure of this paper follows: Photovoltaic Description in section II, Maximum Power Point Tracking in Section III. In Section IV, Boost Converter is obtained. The IM Mathematical Model is given in section V. Vector Control Technique in Section VI. Space Vector PWM in section VII. Diode Clamp Inverter in section VIII. Wavelet Physical Layer Based in Section IX Simulation results is given in Section X. Finally, Section XI gives a conclusion.

2. Photovoltaic description

The objective of PV cells is the light conversion into electricity using materials that exhibit the effect. Nowadays PV energy that solar has become power. The power conditioner (PC) is a very important stage in the PV complete control system to convert (DC/DC) or (DC/AC) to drive the IM in the last stage as can be seen in Fig.1.

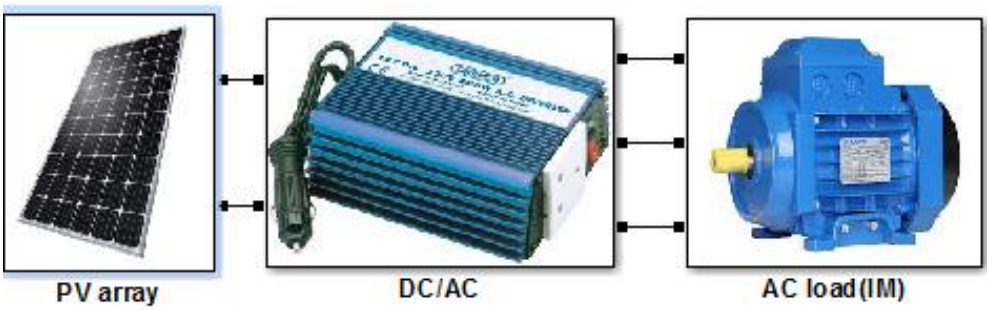


Fig. 1: PV Control System Circuit.

The efficiency of the PV modules is low and the MPPT can be obtain from highly PC design to extract optimal PV module response. Various factors affects the cell conversion efficiency such as [15].

- Reflectance efficiency,
- Thermodynamic efficiency,
- Charge carrier separation efficiency,
- Conduction efficiency values.

The amount of energy produced by PV module related to angle of inclination, climatic factors, inverter characteristics, and system-grid coupling [16]. The overall performance of solar cell varies with varying Irradiance and Temperature. With the change in the time of the day the power received from the Sun by the PV panel changes. Not only this both irradiance and temperature affect solar cell efficiency as well as corresponding Fill factor also changes [17].

In design of any PV array all the above properties should be taken in consideration. Practically PV has nonlinearity effect due to the behaviour of diode and nonlinearity effects in the other parts .The PV cell internal combustion can be shown in Fig.2.

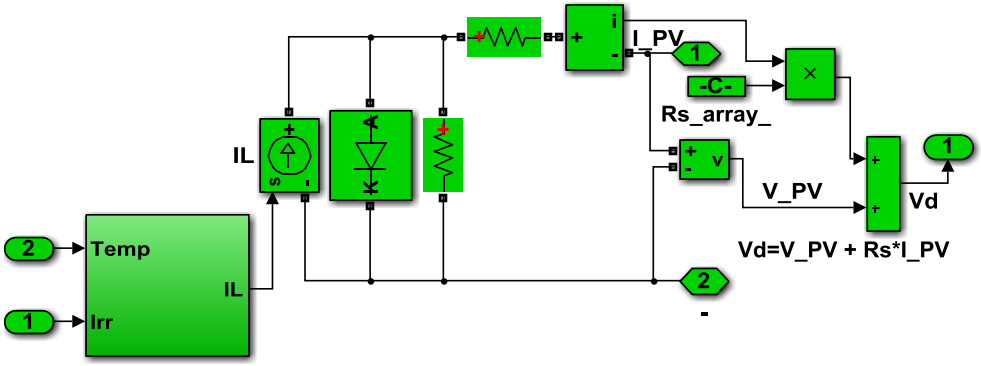


Fig. 2: PV Cell Internal Configuration.

To increase the voltage, single PV panels is connected in series and for high current, the PV panels is connected in parallel to produce the desired power output [18].

The series array resistance can be calculated as:

$$R_{S_array} = R_s * \frac{N_{series}}{N_{parallel}} \quad (1)$$

The series resistance comes from the following

- Resistance of the metal contacts
- Ohmic losses in the front surface of the cell
- Impurity concentrations
- Junction depth

The parallel array resistance can be calculated with 0.05 compention as:

$$R_{P_array} = 0.05 * S_{ref} \quad (2)$$

And its approximately equal to changing in revere bias voltage to changing in the reverse bias current of the diode characteristic.

Where

S is the irradiance

The diode voltage can be calculated as in (3)

$$V_{diode} = V_{pv} + R_s I_{pv} \quad (3)$$

The Diode characteristic which is depends on various variables give it the nonlinearity characteristic is given in (4)

$$I_{diode} = I_{out} * [Exp(V_{diode} / V_T) - 1] \quad (4)$$

Where

I_{out} , is the current that flows in the reverse direction when the diode is reverse biased. It is called as the leakage current or saturation current.

VT is the temperature voltage and its can be illustrated as in (5)

$$V_T = K * T_{pv_cell} / q * N_{Ident} * N_{cells} * N_{series} \quad (5)$$

Where

N_{ident} is the diode ideality factor and it's an indicator of the behavioral proximity of the device under test, to an ideal diode.
q=1.6e-19C is the electron charge,
K=1.38e-23 j/k is the Boltzmann's constant.
The load current Simulink implementation circuit is shown in Fig.3.

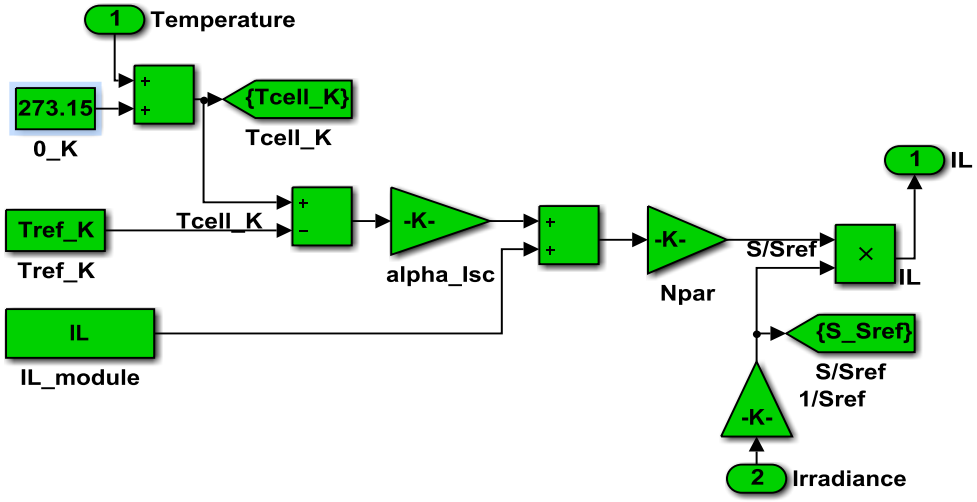


Fig. 3: The Load Current Simulink Circuit.

The load current can be expressed in the (6)

$$I_L = \frac{S}{S_{ref}} * (I_{L_Ref} + \alpha * (T_{pv} - T_{ref}),\ \alpha = 0.001 \quad (6)$$

The PV cell voltage and current generated, is expressed in (7):

$$V_g = I_g R_s (N_s / N_p) lin(1 + \frac{N_p I_{ph} - I_g}{N_p I_o}) \quad (7)$$

$$I_g = I_{ph} - I_o (\mathrm{Exp}(qV_g / kT) - 1) \quad (8)$$

Fig.3 shows the (V-I) limits of the PV panel so it can protect when the operation conditions is short circuit current or open circuit voltage.
From (9) and when we set Vg =0 in the exponential expression, hence the short circuit current can be obtained as:

$$I_{sc} = I_{ph} \quad (9)$$

The open circuit voltage is obtained by equating the cell current is to zero and can be expressed as in (10).

$$V_{sc} = (kT / q) lin(\frac{I_{ph} + I_o}{I_o}) \cong (kT / q) lin(\frac{I_{ph}}{I_o}) \quad (10)$$

In this equation the value of $I_{ph} >> I_o$
The MPP of the PV cell can be expressed as:

$$P_m = I_m V_m = FF * I_{sc} V_{sc} \quad (11)$$

Where
FF, Im,Vm is the fill factor which is the reliability indictor, maximum current and maximum voltage respectively.

$$FF = P_{max} / P_{theoretical} \quad (12)$$

The efficiency of the PV panel which is the ratio of the electrical power output POUT, compared to the solar power input, PIN, can be calculated as:

$$\eta = P_{out} / P_{in} \quad (13)$$

$$P_{out} = P_{max} (W / m^2) \quad (14)$$

For AM 1.5, P_{in} = 1000 (W/m^2)

3. Maximum power point tracking

The efficiency increasing of the PV cell is very import factor so a MPPT algorithm is required to ensure optimal demand of solar energy conversion [19].
Normally the solar energy conversion systems are operated either at MPP or at LPP [20].
The incremental conductance MPPT operation as in [21]. The three most common MPPT algorithms are:

- Perturbation and observation (P&O).
- Incremental conductance, the voltage remains constant with this algorithm and its used in this paper to ensure better regulation of the output which is mean better duty cycle correction for sufficient stabilization of DC voltage. Simulink implementation of the duty cycle can be shown in Fig.4.
- Fractional open-circuit voltage.

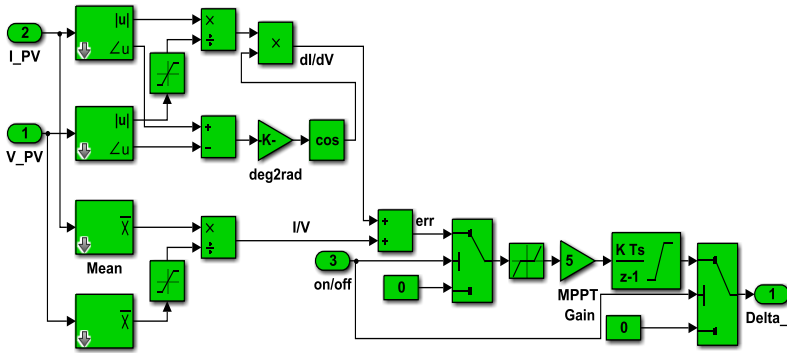


Fig. 4: Duty Cycle Correction Due to MPPT.

4. Boost converter

The increase of the power density is the one of the most important design due to the physical limitation such as space and weight [22]. There are three types of categories (buck converters, boost converters and buck boost converters).

The boost converter is applied in many power (DC-DC) conversion systems, such as PV power conditioning systems, communication, control systems. The boost converter is used because the output voltage is always high with respect to source voltage. The boost inductor in the boost converter is the main component of the converter [23]. The characteristics of the boost converter is very important to combined with PV control circuit between the PV array and the input of the inverter to stabilize the DC voltage. This is to force the PV array to deliver the maximum power to the load [24]. The duty cycle control is important factor to verify MPPT algorithm.

5. IM Mathematical model

PV systems have been used in many industrial applications. The harmonic sources like the renewable energy sources produce electric power to the load which is directly connected to cells [25]-[26].the mathematical model of the IM in the dq- reference frame.

$$\begin{bmatrix} i_{sd} \\ i_{sq} \\ i_{rd} \\ i_{rq} \end{bmatrix} = \frac{1}{L_m{}^2 - L_s L_r}\left(A \begin{bmatrix} i_{sd} \\ i_{sq} \\ i_{rd} \\ i_{rq} \end{bmatrix} + \begin{bmatrix} L_s & 0 & L_m & 0 \\ 0 & L_r & 0 & L_m \\ L_m & 0 & L_r & 0 \\ 0 & L_m & 0 & L_r \end{bmatrix} * \begin{bmatrix} v_{sd} \\ v_{sq} \\ v_{rd} \\ v_{rq} \end{bmatrix}\right)$$

$$A = \begin{bmatrix} \frac{-(R_s + R_r(L_m/\tau_r)^2)}{\sigma L_s} & 0 & \frac{L_m}{\sigma L_s L_r \tau_r} & \frac{\omega_r L_m}{\sigma L_s L_r} \\ 0 & \frac{-(R_s + R_r(L_m/\tau_r)^2)}{\sigma L_s} & \frac{-\omega_r L_m}{\sigma L_s L_r} & \frac{L_m}{\sigma L_s L_r \tau_r} \\ L_m/\tau_r & 0 & -1/\tau_r & -\omega_r \\ 0 & L_m/\tau_r & \omega_r & -1/\tau_r \end{bmatrix}$$

$$B = \begin{bmatrix} \frac{1}{\sigma L_s} & 0 \\ 0 & \frac{1}{\sigma L_s} \\ 0 & 0 \\ 0 & 0 \end{bmatrix}, C = \begin{bmatrix} 1 & 0 & 0 & 0 \\ 0 & 1 & 0 & 0 \end{bmatrix}$$

Where

Ls, Lr, Lm, σ, tr, and wr are the stator inductance, rotor inductance, mutual inductance, leakage coefficient, rotor time constant, motor angular velocity (rad/s) respectively.

Simulink implementation of IM Electrical part can be shown as in Fig.5.

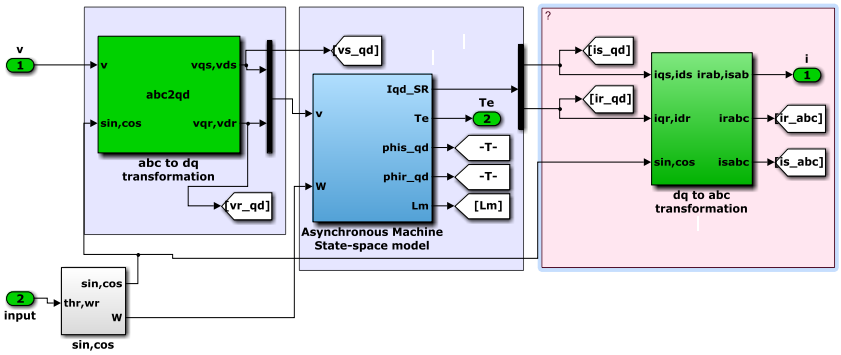


Fig. 5: Electrical Part of the IM.

The mechanical part of the IM can be derived from the torque T_e which is a function of the stator fluxes and currents, thus.

$$T_e = \left(L_s i_{ds} + L_m i_{dr}\right) I_{qs} - \left(L_s i_{qs} + L_m i_{qs}\right) I_{ds} \quad (17)$$

$$\varphi_{qr} = L_r i_{qr} + L_m i_{qs} \quad (18)$$

$$\varphi_{dr} = L_r i_{dr} + L_m i_{ds} \quad (19)$$

$$v = Ri + d\varphi/dt + W\varphi \quad (20)$$

$$\varphi = Li$$

Where:
R, L, W= [4x4] diagonal matrix of the winding resistances, self and mutual inductances, depends on the rotor speed w_r in d- q axis respectively.

v, I,φ= [4x1] stator and rotor dq-axis voltage vector, current vector, flux linkage vector
As in the electrical part, the mechanical part of the IM. Using discrete forward Euler trapezoidal integration to complete mechanical part of the IM as can be shown in Fig.6.

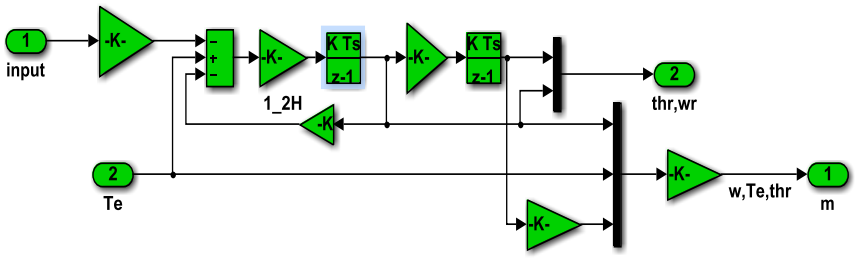


Fig. 6: Mechanical Part of the IM.

6. Vector control technique

The vector control principle as one part of field oriented control (FOC) to control the torque and speed in individual way. Fig.7 shows the principle of alpha-beta, rotation around the d-q coordinate in stationary reference frame [27].

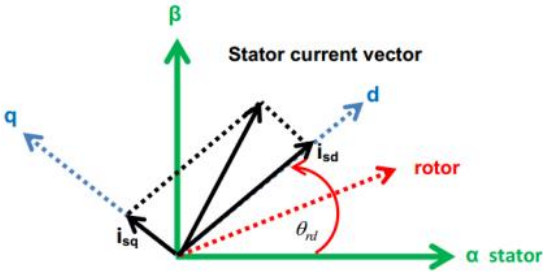


Fig. 7: Stationary Reference of Vector Control.

In this paper new vector is introduced depending on the wavelet error along with actual speed to generate the diode clampled multilevel inverter pulses according to the SVPWM as can be seen in Fig.8.

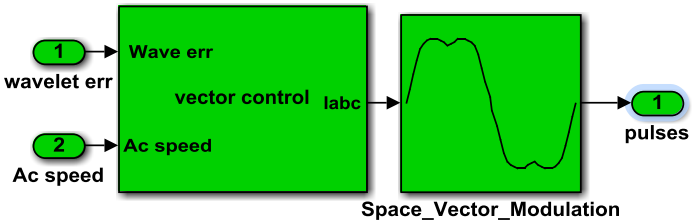


Fig. 8: Vector Control with SVPWM Simulink Implementation.

7. Space vector PWM

In the mid of 1980s new PWM technique is developed to increase the duty cycle of the convetional PWM from (78-99%) this called SVPWM. In SVPWM method, the reference voltage vector is approximated using a combination of the eight switching patterns denoted by V0, V60, V120, V180, V240, V300, Org000 and Org111[28].
A 3-φ mathematical system can be represented by a space vector a of three-phase voltages. The space vector can defined as in [29].

$$v(t) = 1.5[v_a \exp(j0) + v_b \exp(2/3j) + v_c \exp(4/3j)] \quad (21)$$

Where
Va,Vb,Vc is sinusoidal amplitude voltages
To control the Gate drive converter SVPWM technology and currently implements FOC. In this paper instead of using 12 gate dive just 6 gates drives of IR2110 gate drives ure used to control the 12 IGBT transistors as can be seen in the Fig.9.

The IR2110 is high voltage, high speed power IGBT driver with independent high and low side referenced output channels [30]. Proprietary HVIC and latch immune CMOS technologies enable ruggedized monolithic construction. The output drivers feature a high pulse current buffer stage designed for minimum driver cross-conduction. Propagation delays are matched to simplify use in high frequency applications [31]-[32].

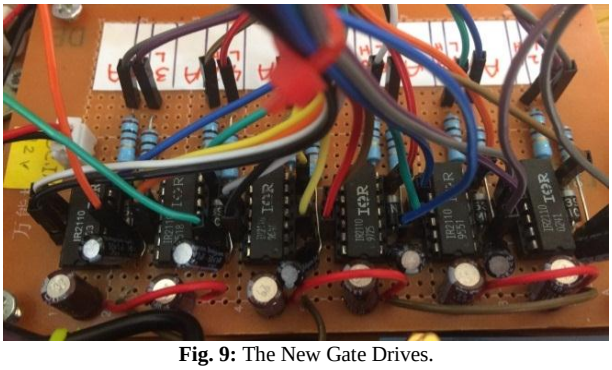


Fig. 9: The New Gate Drives.

The typical connection of each gate drive can be shown as in Fig.10.

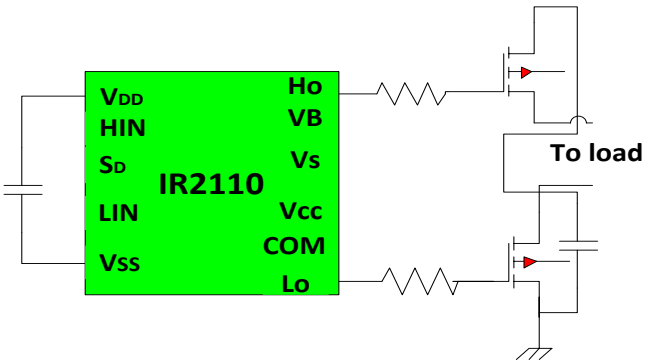


Fig. 10: IR2110 Gate Drive Typical Connection.

8. Diode clamped inverter

3-φ LPC inverter topology is implemented by using the Simulink single phase may be shown in Fig.11.

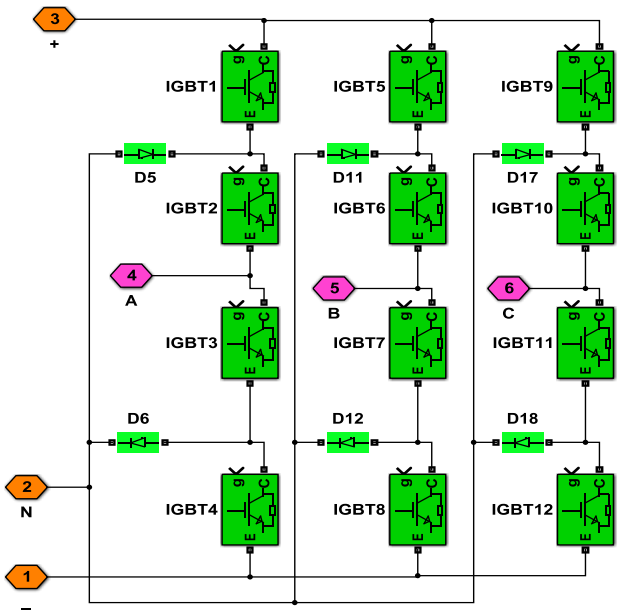


Fig. 11: Diode Clamped Invereter Connection.

The hardware implementation of the NDC can be shown in Fig.12. In this configuration, 12 IGBT of IRG4PH50UD with 6 diodes are used due to the following resons:

- Ultra-Fast: Optimized for high operating frequencies up to 40 kHz in hard switching and (>200 kHz) in resonant mode.
- New IGBT design provides tighter parameter distribution and higher efficiency than previous generations.
- IGBT co-packaged with HEXFREDTM ultrafast, ultra-soft-recovery anti-parallel diodes for use in bridge configurations.
- Industry standard TO-247AC package [33].

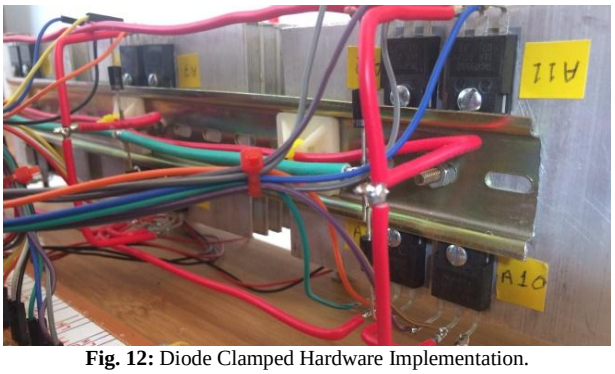


Fig. 12: Diode Clamped Hardware Implementation.

The main components of the hardware implementation can be shown in Fig.13.

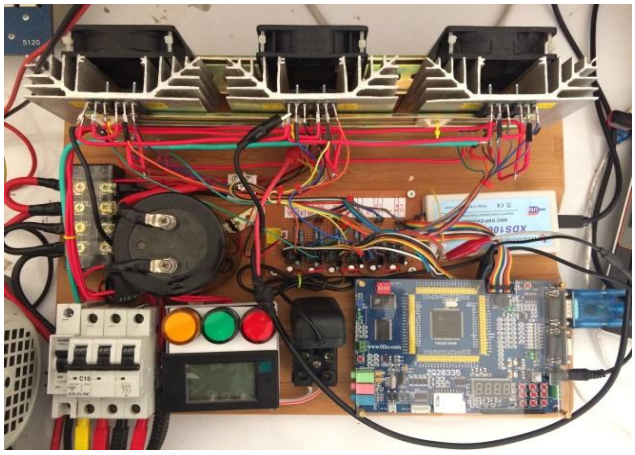


Fig. 13: Topveiw of the Main Hardware Implementation.

The complete Simulink diode clamped with control signal is shown in Fig.14.

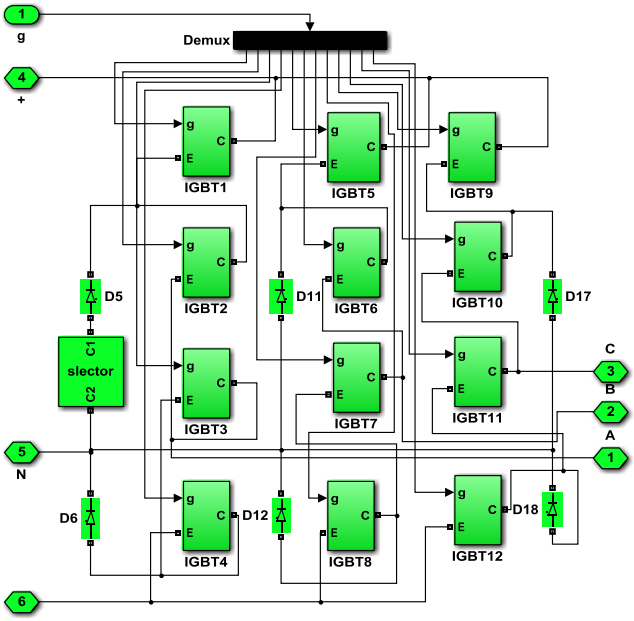


Fig. 14: Diode Clamped Invereter Complete Circuit.

9. Wavelet physical layer based

A wavelet can be defined as a waveform of limited duration that has zero average value. Wavelet transform techniques currently provide the most promising approach to high-quality image compression. The advanced signal processing techniques make it easy

to work in various regions. The physical layer consists of the electronic circuit combined with the vector control.
The physical layer provides an electrical, mechanical interface to the IM for the feature extraction. The properties of the electrical output signals, the frequencies are similar to the low level parameters [34]-[35].
Wavelets are adapted to local properties of functions to a larger extent than the Fourier basis. The discrete wavelet transforms (DWT) is given by [36].

$$\psi_{m,n}(t) = a_0^{-m/2}\psi\left(\frac{t - nb_0a_0^{m}}{a_0^{m}}\right) \quad (22)$$

The most important property is the regularity condition and it can be expressed in the following formula [37].

$$\int \frac{|\psi(\omega)|^2}{|\omega|} d\omega < +\infty \quad (23)$$

The minimum error selection depends on the energy of each level in wavelet and can be calculated according to (24):

$$Energy\ of\ \ selected\ level = \int (selected\ level\ signal)dt \quad (24)$$

The number of wavelet decomposition levels used in (25) was performed according to the following criteria:

$$Wdecomp = \frac{\log(fs/f)}{\log(2)} \pm 1 \quad (25)$$

Where fs is the sampling frequency (10 kHz) and f is source frequency [38].

10. Simulation results

To investigate the proposed algorithm, the Simulink program has been use to model the IM, Diode clamped inverter, vector control, wavelet, MPPT unit with Incremental Conductance algorithm, boost converter to ensure better evaluation of the proposed algorithm. The proposed algorithm can be shown in Fig.15.

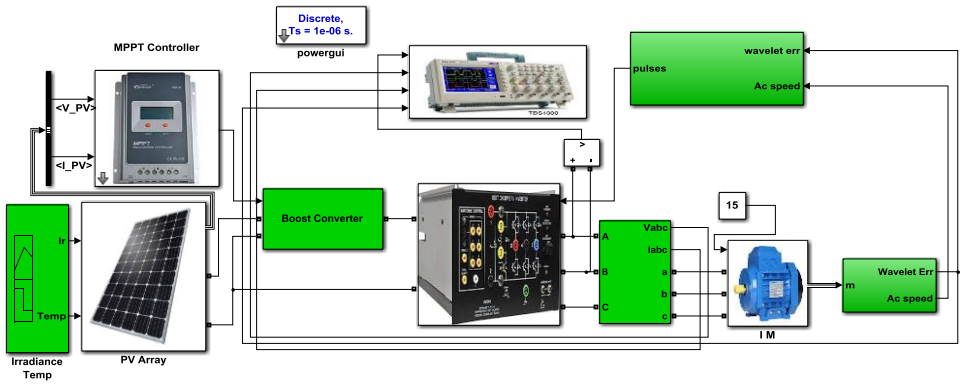


Fig. 15: Simulink Proposed Circuit.

Matlab/Simulink toolbox is used to model the PV panel. Implements a PV array built of strings of PV modules connected in parallel. Each string consists of modules connected in series [39].
For Sun Power PL panel in with 1000W/m2 and for 0.25 W/m2 without and with SC, the (V-I) and (P-V) response can be shown in Fig.16.

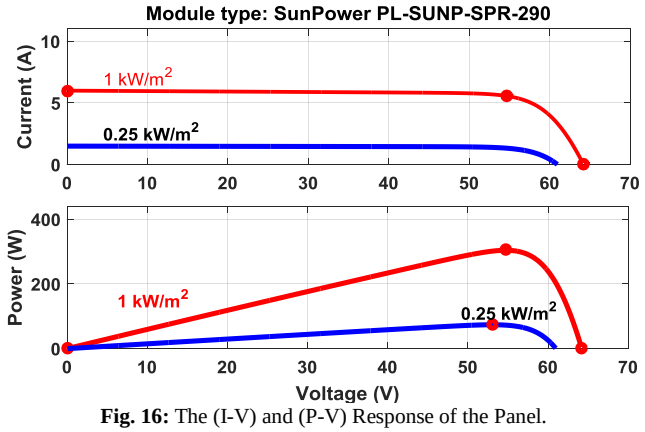


Fig. 16: The (I-V) and (P-V) Response of the Panel.

With complete module under [0 25 50 75] Co, the (V-1) and (P-V) characteristic can be shown in Fig.17.
In this Figure, The MPPT is occurs at 25 C0 and the power around 7.5kW.

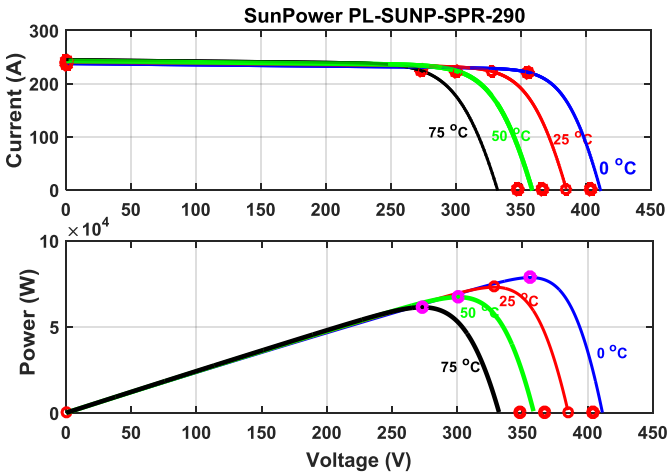


Fig. 17: MPPT and Current for 40 PV Arrays.

The error recording is recorded in Table 1.

Table 1: Error of PL-SUNP-SPR-290 PV Array

Error term	Value
Error $V_{open\ circuit}$	-0.05 %
Error $I_{short\ circuit}$	0.66 %
Error $V_{max\ power}$	0.01 %
Error $I_{max\ power}$	-0.36 %

The complete hardware set up can be shown in Fig.18.



Fig. 18: Complete Setup of the Proposed Work.

The specification of the complete reading is manifested in Table 2.

Table 2: Parameters of the Solar Panels

Solar system parameter	Value	Unit
DC side MPP voltage	8.85	V
MPP current	5.8	A
Open-circuit voltage	65	V
Short-circuit current	6	A
Temperature	25	°C
Solar irradiance	1000	W/m
Diode saturation current I0 (A)	6e-12	A
Diode ideality factor	0.9	
AC side Rated grid voltage	230	V
Light-generated current IL	5.8	A
Filter capacitor	1200	µF
Switching frequency	20	kH
Inductor filter	5e-3	H

At beginning the with 0.7 threshold, Haar wavelet is developed to get the wavelet error to be used vector control as can be shown in Fig.19.
At this stage sufficient operation of MPPT algorithm is verified.

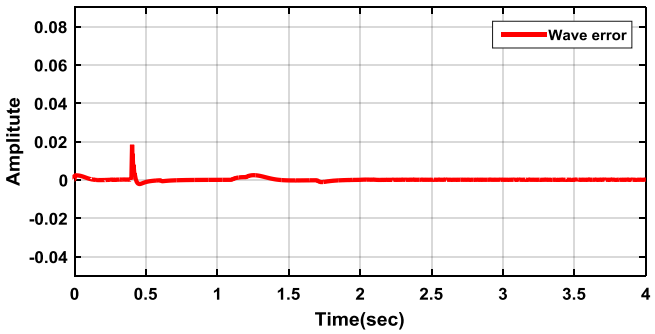


Fig. 19: Haar Wavelet Error.

The corresponding actual speed and SVPWM with unsmooth operation before 0.5 sec is given in Fig.20 and Fig.21 respectively.

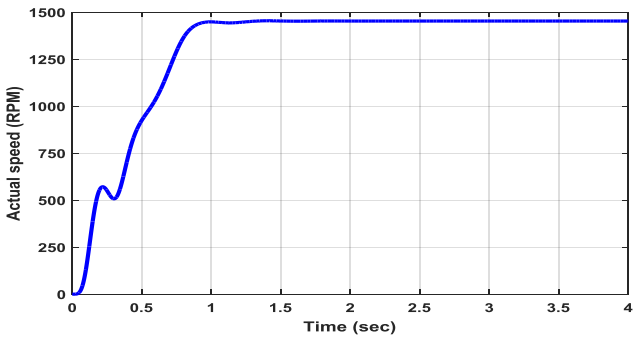


Fig. 20: Actual Speed with Haar Wavelet.

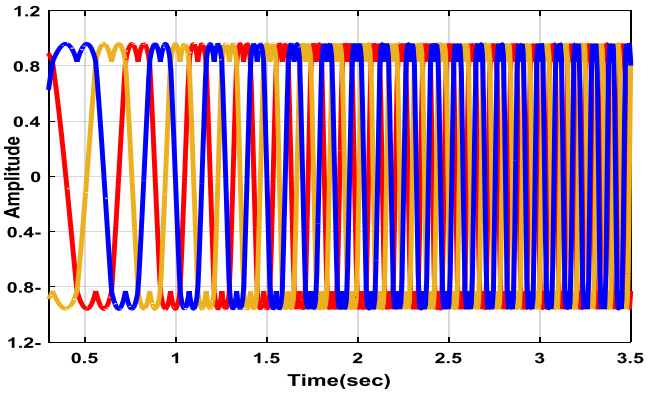


Fig. 21: SVPWM with Haar Wavelet.

The DC voltage generated by MPPT can be shown in Fig.22.

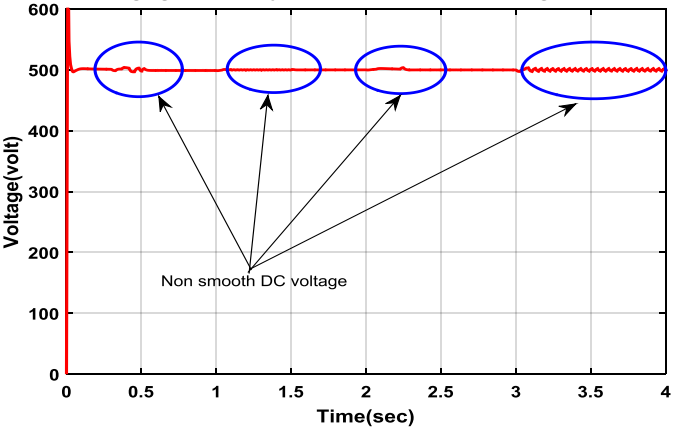


Fig. 22: DC Voltage with First Haar Wavelet.

To ensure best operation of the proposed algorithm, new adaptive wavelet is developed with zero error as can be seen in Fig.23.

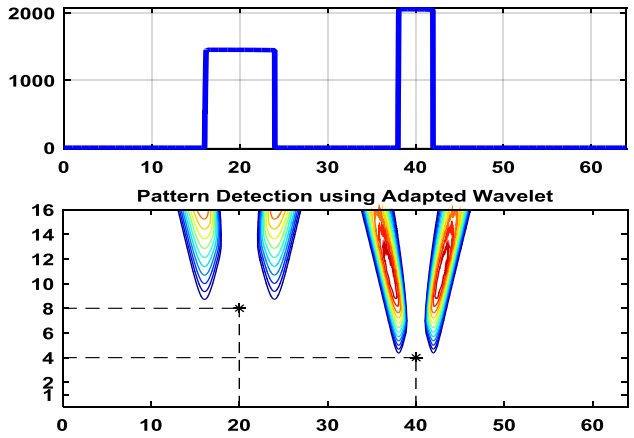


Fig. 23: New Adaptive Wavelet Development.

The corresponding actual speed and wavelet error (green) can be shown in Fig.24. Considerable improvement is obtained due the new adaptive wavelet organization.

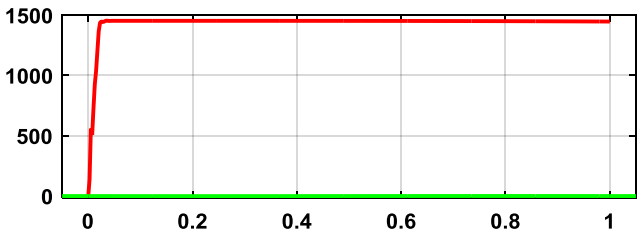


Fig. 24: Actual Speed and Error Due to Adaptive Wavelet.

The current of the IM ensure better smoothing as can be shown in Fig.25.

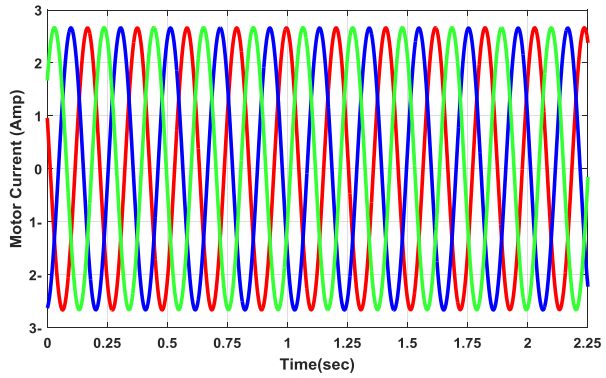


Fig. 25: IM Current Waveform due Adaptive Wavelet.

Smooth DC voltage generated by MPPT in this can be shown in Fig.26.

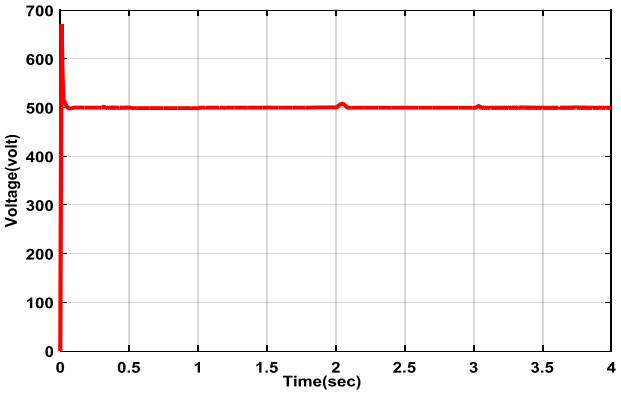


Fig. 26: DC Voltage with Adaptive Wavelet.

11. Conclusions

The signal processing techniques used in this paper are very powerful approach in the PV systems. The performance of the IM is acceptable with combination of vector control and wavelet but still need an improvement especially there are fluctuation in DC voltage generated through the MPPT algorithm and the booster converter. Design new adaptive wavelet instead the conventional Haar wavelet shows better performance specification of IM. SVPWM is new advance in the machine drive especially with the multilevel inverters. Less switching of the gate drive used in this work with F28335 DSP with V3.3 code composer studio as the main part of the computer control strategy.

References

[1] Y. Yi Honga,Angelo A.BeltranJr and A C.Paglinawan, "A robust design of maximum power point tracking using Taguchi method for stand-alone PV system," Applied Energy. vol. 211, pp. 50-63, 2018. https://doi.org/10.1016/j.apenergy.2017.11.041.

[2] U. Laishram and A.M. Nagaraj," Wavelet Modulation for Neutral Point Clamped Multilevel Inverters," International Journal of Emerging Technology and Advanced Engineering, vol.4, no.3, pp61-65, 2014.

[3] A. Chikh and A Chandra," An Optimal Maximum Power Point Tracking Algorithm for PV Systems With Climatic parameters Estimation" IEEE Transactions on Sustainable Energy, vol. 6, no.2, 2015. https://doi.org/10.1109/TSTE.2015.2403845.

[4] G. Li Yi, Jin M.W and A Xiao Chen JieJi. "Application of bio-inspired algorithms in maximum power point tracking for PV systems under partial shading conditions – A review", Renewable and Sustainable Energy Reviews, vol. 81, Part 1, pp 840-873,2018. https://doi.org/10.1016/j.rser.2017.08.034.

[5] C. Huang, Long Wang, Ryan Shun, Cheung Yeung ,Zijun Zhang ,Henry Shu, H Chung and A Bensoussan," A Prediction Model-Guided Jaya Algorithm for the PV System Maximum Power Point Tracking," IEEE Transactions on Sustainable Energy ,vol.9, no. 1, 2018. https://doi.org/10.1109/TSTE.2017.2714705.

[6] M. Makhlouf, F Messai and H Benalla, "Vectorial Command of Induction Motor Pumping System Supplied by a Photovoltaic Generator," Journal of Electrical Engineering, v62, no.1,2011. https://doi.org/10.2478/v10187-011-0001-7.

[7] K. Tahir, C Belfedal,T Allaoui,M Denai and M Doumi," A new sliding mode control strategy for variable-speed wind turbine power maximization,"Int Trans Electr Energ Syst. 2018;e2513. https://doi.org/10.1002/etep.2513.

[8] A. M. S. Furtado, Fabricio Bradaschia, Marcelo C. Cavalcanti and L R. Limongi ,"A Reduced Voltage Range Global Maximum Power Point Tracking Algorithm for Photovoltaic Systems Under Partial Shading Conditions," IEEE Transactions on Industrial Electronics , vol.65, no. 4, 2018. https://doi.org/10.1109/TIE.2017.2750623.

[9] Z. Wu and D Yu," Application of improved bat algorithm for solar PV maximum power point tracking under partially shaded condition," Applied Soft Computing, vol.62, pp101-109, 2018. https://doi.org/10.1016/j.asoc.2017.10.039.

[10] C. Eddine Feraga and A Bouldjedri," Performance of a Photovoltaic Pumping System Driven by a Single Phase Induction Motor Connected to a Photovoltaic Generator," ATKAFF, vol. 57, no.1, pp.163–172, 2016.

[11] S. Yang, A. Bryant, P. Mawby, D. Xiang, L. Ran, and P. Tavner, "An industry-based survey of reliability in power electronic converters," IEEE Trans. Ind. Appl., vol. 47, pp. 1441-1451, 2011. https://doi.org/10.1109/TIA.2011.2124436.

[12] Markus Andresen, Ke Ma, G Buticchi, J Falck, F Blaabjerg and M Liserre." Junction Temperature Control for More Reliable Power Electronics," IEEE Transactions on Power Electronics, vol.33, no.1, 2018. https://doi.org/10.1109/TPEL.2017.2665697.

[13] F. Jeng Lin, S Gang Chen, Y Tsen Liu and S Yao Chen," A power perturbation-based MTPA control with disturbance torque observer for IPMSM drive system," Transactions of the Institute of Measurement and Control,2018.

[14] M. Arrouf and N. Bouguechal," Vector control of an induction motor fed by a photovoltaic generator," Applied Energy, vol. 74, pp159–167,2003. https://doi.org/10.1016/S0306-2619(02)00142-3.

[15] https:/ /energy. gov /eere/ solar/articles/solar performance and efficiency

[16] J. Jesús Quinones, and P.K. Nair," Comparative study of system performance of two 2.4 kW grid-connected PV installations in Tepic-Nayarit and Temixco-Morelos in México," Energy Procedia, vol.57, pp161 – 167,2014. https://doi.org/10.1016/j.egypro.2014.10.020.

[17] P. Arjyadhara, Ali S.M and J Chitralekha," Analysis of Solar PV cell Performance with Changing Irradiance and Temperature," International Journal of Engineering and Computer Science, vol.2, no.1, pp 214-220, 2013.

[18] http://www.alternative-energy-tutorials.com/solar-power/pv-array.html.

[19] N. H Armghan, Iftikhar, A Ammar Armghan and S M Arsalan,"Back stepping based non-linear control for maximum power point tracking in photovoltaic system," Solar Energy, vol.159, pp 134-141,2018. https://doi.org/10.1016/j.solener.2017.10.062.

[20] S. Lyden and M. E. Haque," Maximum power point tracking techniques for photovoltaic systems: A comprehensive review and comparative analysis, Renew," Sustain. Energy Rev., vol. 52, pp. 1504-1518, 2015. https://doi.org/10.1016/j.rser.2015.07.172.

[21] J. Kivimäki, S Kolesnik, M Sitbon, T Suntio and A Kuperman," Design Guidelines for Multi-loop Perturbative Maximum Power Point Tracking Algorithms," IEEE Transactions on Power Electronics,vol. 33, no. 2, 2018. https://doi.org/10.1109/TPEL.2017.2683268.

[22] A. B. Ponniran, K. Matsuura, K. Orikawa and J. Itoh, "Size reduction of DC-DC converter using flying capacitor topology with small capacitance", IEEJ J. Ind. Appl., vol. 3, no. 6, pp. 20-30, 2014. https://doi.org/10.1541/ieejjia.3.446.

[23] H. Nam Le and J Ichi Itoh," Wide-Load-Range Efficiency Improvement for High-Frequency_SiC-Based Boost Converter with Hybrid Discontinuous Current Mode," IEEE Transactions on Power Electronics, vol.33, no.2, 2018. https://doi.org/10.1109/TPEL.2017.2689822.

[24] K. S. Gaeid ,"Space vector Modulation for V/f Induction Motor Control ," Wulfenia, vol. 20 ,no.3,pp. 166-178,2013.
[25] C. Rodriguez and G.A.J. Amaratunga, "Comparison Between Frequency-Matched and True Sine Wave Grid-Connected Photovoltaic Modules," in Proc. 6th WSEAS International Conference on Power Systems, Portugal, pp.1317-1322, 2006.
[26] J. Klima, "Closed Form Analytical Investigation of Space-Vector PWM Inverter Fed Induction Motor Drive under DC-Bus Voltage Pulsation," WSEAS Transactions on Power Systems, vol.3, no.3, pp.63-75, 2008. https://doi.org/10.1109/ICELMACH.2008.4800208.
[27] K. S Gaeid, HW Ping and HAF Mohamed," Indirect vector control of a variable frequency induction motor drive (VCIMD)," Instrumentation, Communications, Information Technology, and Biomedical, 2009. https://doi.org/10.1109/ICICI-BME.2009.5417273.
[28] K Sravanthi and M RanjithS Srinivasulu," Space Vector Pulse Width Modulation Based Indirect Vector Control of Induction Motor," International Journal of Innovative Research in Advanced Engineering (IJIRAE), no.1, vol2,pp281-290,2015.
[29] S. Bindu,Vinod and V. Thomas," Detection of Static Air-Gap Eccentricity in Three-Phase Squirrel Cage Induction Motor Through Stator Current and Vibration Analysis," Advances in Power Systems and Energy Management ,pp 511-518,2018. https://doi.org/10.1007/978-981-10-4394-9_50.
[30] https://www.infineon.com/dgdl/ir2110.pdf.
[31] M. Ayyub Khan, T Hasan, A Ali Moinuddinand and E Khan," Physical Layer Unequal Error Protection of Wavelet Coded Video Using Hierarchical QAM," IEEE Symposium on Industrial Electronics and Applications, Penang, Malaysia pp217-221,2010. https://doi.org/10.1109/ISIEA.2010.5679468.
[32] http://www.irf.com/productinfo/datasheets/data/irg4ph50ud.pdf.
[33] I,Shisharama," Fundamentals of Sensor Network Programming," Wiley,2010.
[34] Saffor, Amhamed; Ramli, Abdul Rahman; NG, Kwan-Hoong. A Comparative Study of Image Compression between JPEG and Wavelet. Malaysian Journal of Computer Science, [S. l.], v. 14, n. 1, p. 39-45, june 2001.
[35] N. Onat, S Kiyak and G Gokmen, "Experimental Wavelet Transient-State Analysis of Electrical Machines Directly Feeding by Photovoltaic Cells," WSEAS Transactions on Circuits and Systems.no.8, vol.8, pp.719-728, 2009.
[36] K S Gaeid and H Wooi Ping," Wavelet fault diagnosis and tolerant of induction motor: A review ,"International Journal of the Physical Sciences, vol. 6,no.3, pp. 358-376, 2011.
[37] K S Gaeid and H Ping, W., Khalid, M.,and A. Masaoud, "Sensor and Sensorless Fault Tolerant Control for Induction Motors Using a Wavelet Index," Sensors, vol. 12, no.4, pp. 4031-4050, 2012. https://doi.org/10.3390/s120404031.
[38] G. Brando,L Piegari and I Spina," Simplified Optimum Control Method for Monoinverter Dual Parallel PMSM Drive," IEEE Transactions on Industrial Electronics,vol.65, no.5, 2018. https://doi.org/10.1109/TIE.2017.2758751.
[39] SM Alghuwaine," Application of a DC chopper to maximize utilization of solar-cell generators, "IEEE/PES, winter meeting, New York, 1991.